Spatial organization of an enzyme cascade in Ni-ZIF-8 framework for efficient sugar nucleotide synthesis

Youbo Yu[1], Xingcheng Zhou[1], Lisha Yan[1], Jie Hong[2], Li Yang[3], Krongthong Kamonsuangkasem[4], Peiyi Wang[1], W.M.W.W. Kandegama[1,5], Gefei Hao[1], Libo Zhang[1*]*

1: State Key Laboratory of Green Pesticide, Key Laboratory of Green Pesticide and Agricultural Bioengineering, Ministry of Education, Guizhou University, Guiyang, Guizhou 550025, China

2: Medical College, Guizhou University, Guiyang 550025, China

3: College of Computer Science and Technology, Guizhou University, Guiyang 550025, China

4: Synchrotron Light Research Institute, 111 University Avenue, Muang District, Nakhon Ratchasima, 30000, Thailand

5: Department of Horticulture and Landscape Gardening, Faculty of Agriculture & Plantation Management, Wayamba University of Sri Lanka, Makandura, Gonawila, 60200, Sri Lanka

E-mail:

jhong@gzu.edu.cn

lbzhang@gzu.edu.cn

His_6-BlNahK-SnoopCatcher

MSYYHHHHHHGSGGSGSTESNEVLFGIASHFALEGAVTGIEPYGDGHINTTYLVTTD
GPRYILQQMNTSIFPDTVNLMRNVELVTSTLKAQGKETLDIVPTTSGATWAEIDGGA
WRVYKFIEHTVSYNLVPNPDVFREAGSAFGDFQNFLSEFDASQLTETIAHFHDTPHRF
EDFKAALAADKLGRAAACQPEIDFYLSHADQYAVVMDGLRDGSIPLRVTHNDTKLN
NILMDATTGKARAIIDLDTIMPGSMLFDFGDSIRFGASTALEDEKDLSKVHFSTELFRA
YTEGFVGELRGSITAREAELLPFSGNLLTMECGMRFLADYLEGDIYFATKYPEHNLVR
TRTQIKLVQEMEQKASETHAIVADIMEAARELGSPANLKALEAQKQKEQRQAAEELA
NAKKLKEQLEKGSHMKPLRGAVFSLQKQHPDYPDIYGAIDQNGTYQNVRTGEDGKL
TFKNLSDGKYRLFENSEPAGYKPVQNKPIVAFQIVNGEVRDVTSIVPQDIPATYEFTN
GKHYIT*N*EPIPPK

His_6-PmGlmU-SnoopTag

MHHHHHHKEKALSIVILAAGKGTRMYSDLPKVLHKIAGKPMVKHVIDTVKSIHAKNI
HLVYGHGGEVMQTRLQDEPVNWVLQAEQLGTGHAMQQAAPFFADDENILMLYGD
GPLITAKTLQTLIAAKPEHGIALLTVVLDDPTGYGRIVRENGNVVAIVEQKDANAEQL
KIQEINTGLLVADGKSLKKWLSQLTNNNAQGEYYITDVIALANQDGCQVVAVQASN
FMEVEGVNNRQQLARLERYYQRKQADNLLLAGVALADPERFDLRGELSHGKDVEID
VNVIIEGKVSLGHRVKIGAGCVLKNCQIGDDVEIKPYSVLEEAIVGQAAQIGPFSRLRP
GAALADNTHIGNFVEIKKAHIGTGSKVNHLSYVGDAEVGMQCNIGAGVITCNYDGA
NKFKTIIGDNVFVGSDVQLVAPVTIETGATIGAGTTVTKDVACDELVISRVPQRHIQG
WQRPTKQTKKKLGDIEFI*K*VNK

SnoopCatcher

SnoopTag

The sequence underlined denotes the linker chain connecting BlNahK and SnoopCatcher

The underlined and italic ***N*** and ***K*** are the amino acids for the self-condensation coupling of BlNahK-SnoopCatcher and PmGlmU-SnoopTag, respectively.

Fig. S1 Amino acid sequences of His_6-BlNahK-SnoopCatcher and His_6-PmGlmU-SnoopTag, with key at the bottom.

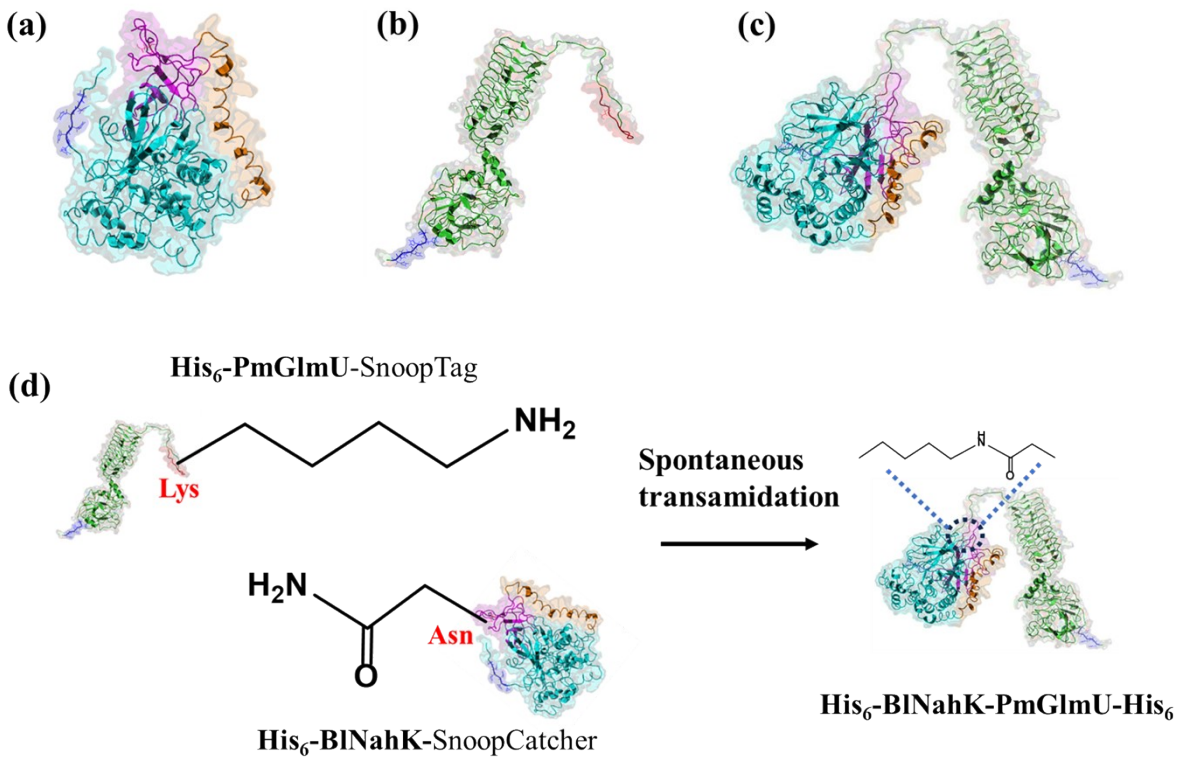

Fig. S2 Structural diagrams of His_6-BlNahK-SnoopCatcher (a), His_6-PmGlmU-SnoopTag (b), and His_6-BlNahK-PmGlmU-His_6 dual-enzyme conjugae (c) and the schemen of spontaneous transamidation reaction that used for dual-enzyme conjugation (d). For (a), cyan denotes the BlNahK, purple denotes the SnoopCatcher linker protein, orange denotes the linker chain connecting BlNahK and SnoopCatcher, and blue denotes the His-Tag. For (b), green denotes the PmGlmU, red denotes the SnoopTag tag, and blue denotes the His_6 tag. For (c), His_6-BlNahK-SnoopCatcher and His_6-PmGlmU-SnoopTag are connected via the side chains of Asn (asparagine) and Lys (lysine) via spontaneous transamidation reaction.

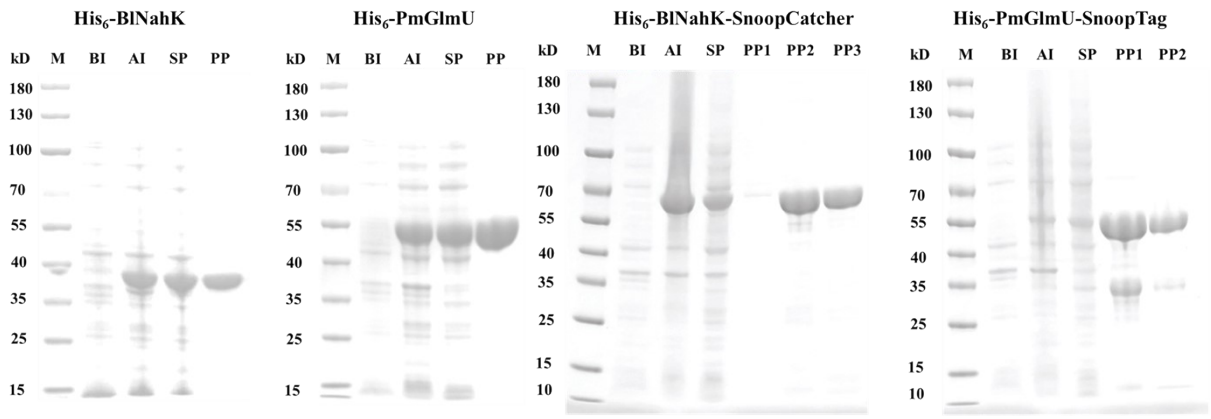

Fig. S3 Protein purification of His_6-BlNahK, His_6-PmGlmU, His_6-BlNahK-SnoopCatcher and His_6-PmGlmU-SnoopTag, where BI denotes the protein before induction, AI denotes the protein after induction, SP denotes the soluble protein, and PP denotes the fractions of purified protein.

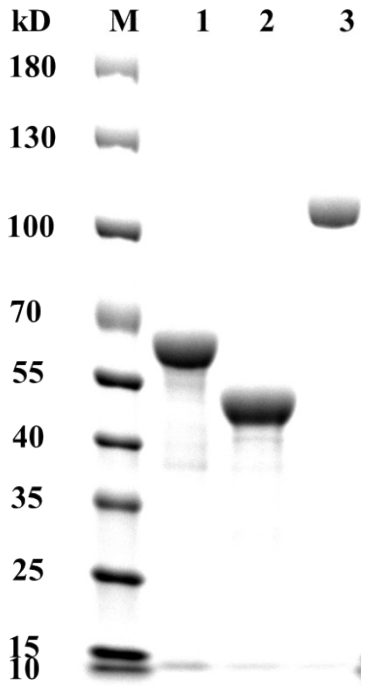

Fig. S4 SDS PAGE analysis of B-P dual-enzyme construction, M: Marker, 1: His_6-BlNahK-SnoopCatcher, 2: His_6-PmGlmU-SnoopTag, and 3: His_6-BlNahK–PmGlmU-His_6.

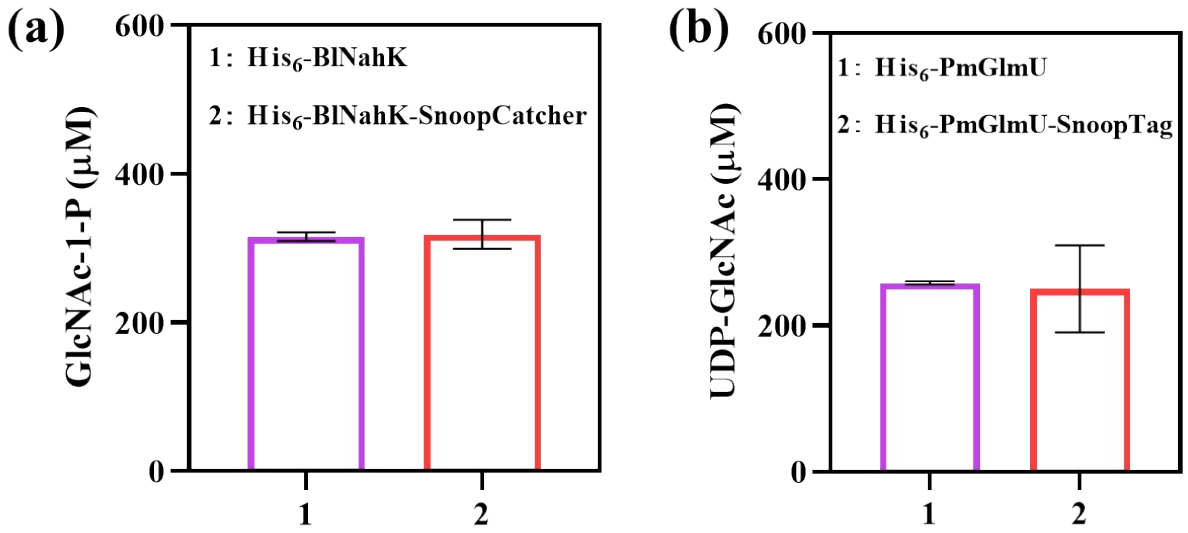

Fig. S5 Activity comparison of His_6-BlNahK and His_6-BlNahK-SnoopCatcher, His_6-PmGlmU and His_6-PmGlmU-SnoopTag. Error bars represent the standard deviation of the mean of duplicate reactions.

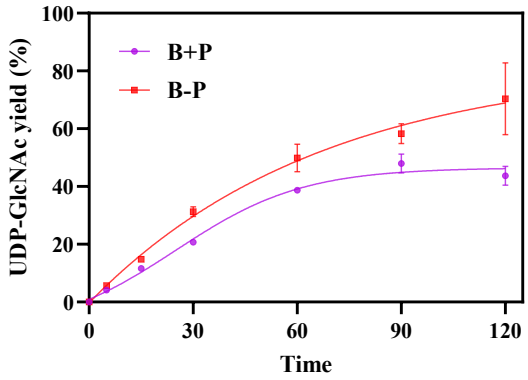

Fig. S6 Activity comparison of B-P dual-enzyme conjugate and B+P free enzymes. Error bars represent the standard deviation of the mean of duplicate reactions.

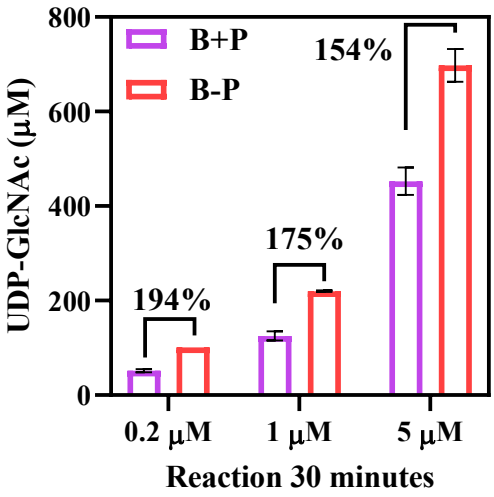

Fig. S7 Activity comparison of B-P dual-enzyme conjugate and B+P free enzymes with different concentrations. 0.2 μM, 1 μM and 5 μM of B-P or each eznyme, 2.4 mM of ATP, 2.4 mM of UTP, 2 mM of GlcNAc, 1 mM $MgCl_2$ were used in a Tris-HCl buffer (pH 8.0, 100 mM), reactions were allowed to proceed for 30 min at 37°C. Error bars represent the standard deviation of the mean of duplicate reactions.

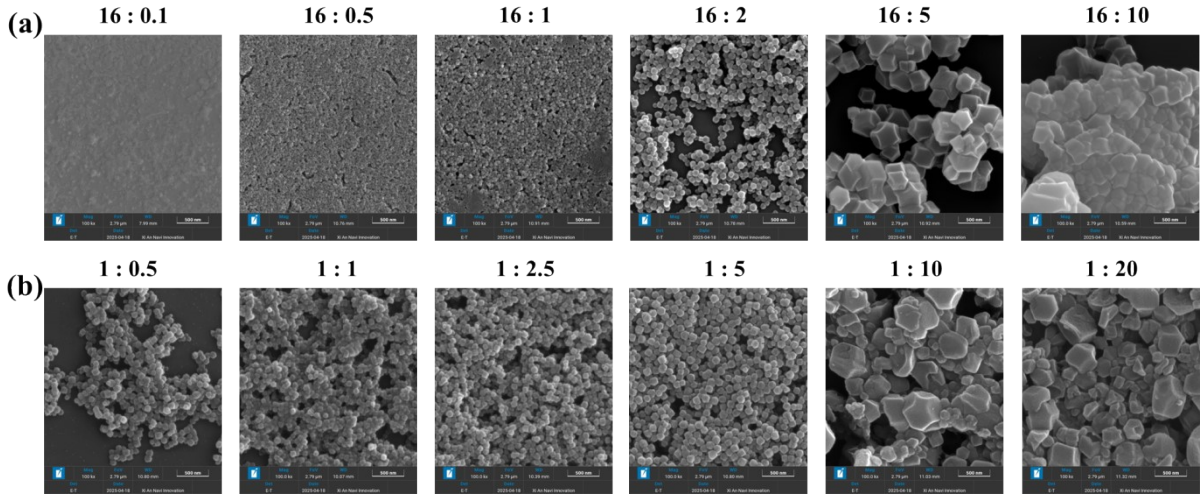

Fig. S8 Condition optimization for ZIF-8 (a) and Ni-ZIF-8 synthesis (b). (a) ZIF-8 nanoparticles are formed by 2-MIM and Zn^{2+} at 0.16 M molar concentrations and different ratios from 16:01 to 16:10, (b) Ni-ZIF-8 nanoparticles were synthesized with a total metal concentration of 0.02 M, by varying the molar ratio of Zn^{2+} to Ni^{2+} from 1:0.5 to 1:20.

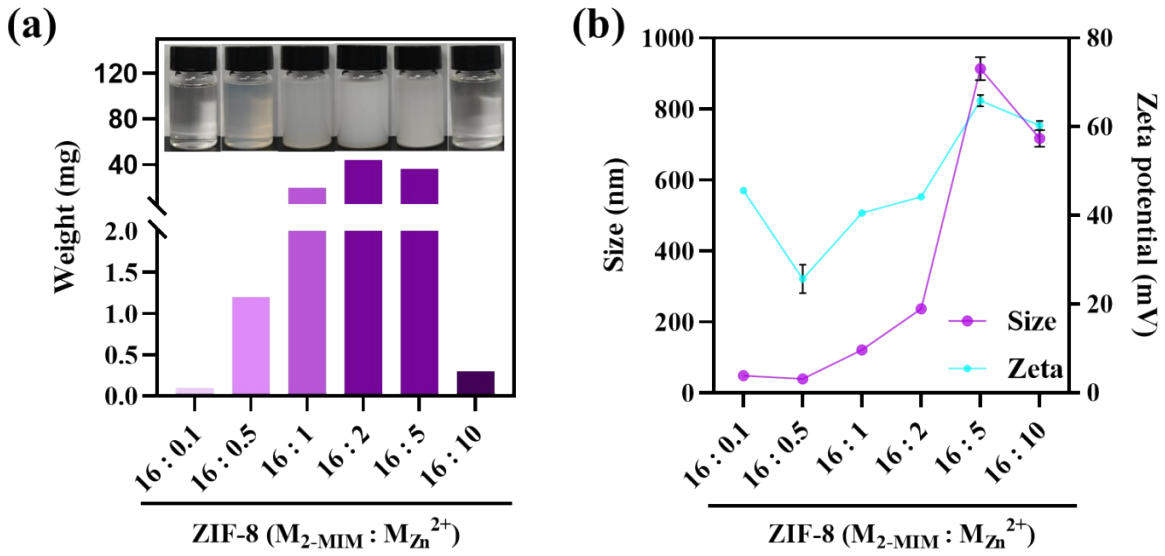

Fig. S9 Yield (a) and DLS analysis(b) of ZIF-8 with different conditions (as described in Fig. S8a), Error bars represent the standard deviation of the mean of duplicate samples.

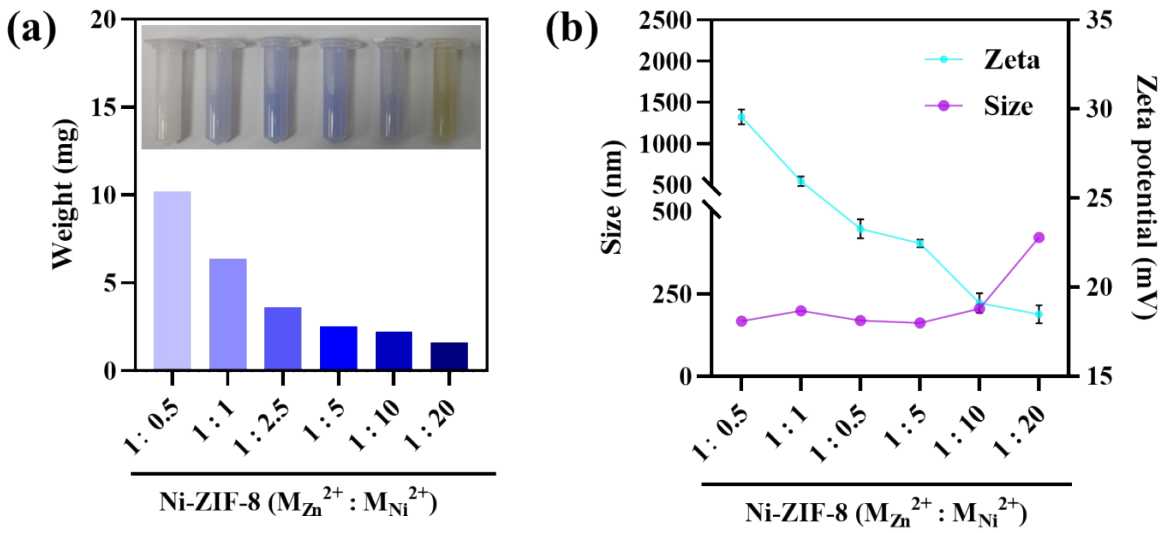

Fig. S10 Yield (a) and DLS analysis(b) of Ni-ZIF-8 with different conditions (as described in Fig. S8b), Error bars represent the standard deviation of the mean of duplicate samples.

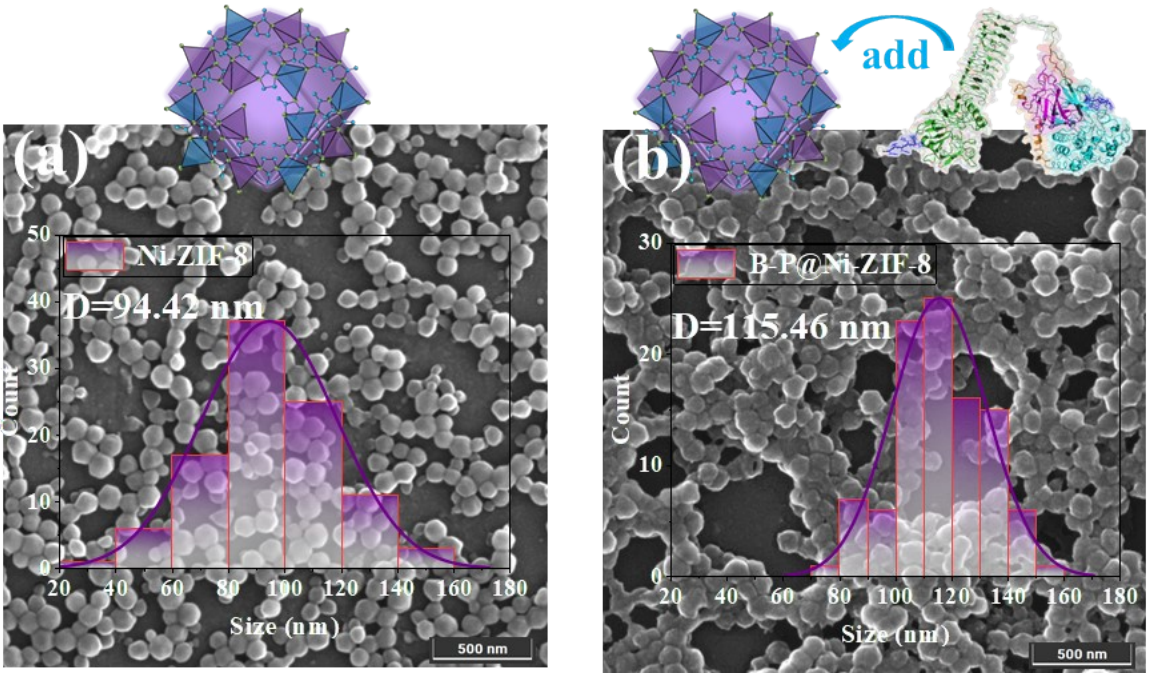

Fig. S11 SEM images and size analysis of Ni-ZIF-8 (a) and B-P@Ni-ZIF-8 (b). For the size alysis, ImageJ was used to caculate the size of 100 particles in each veiw.

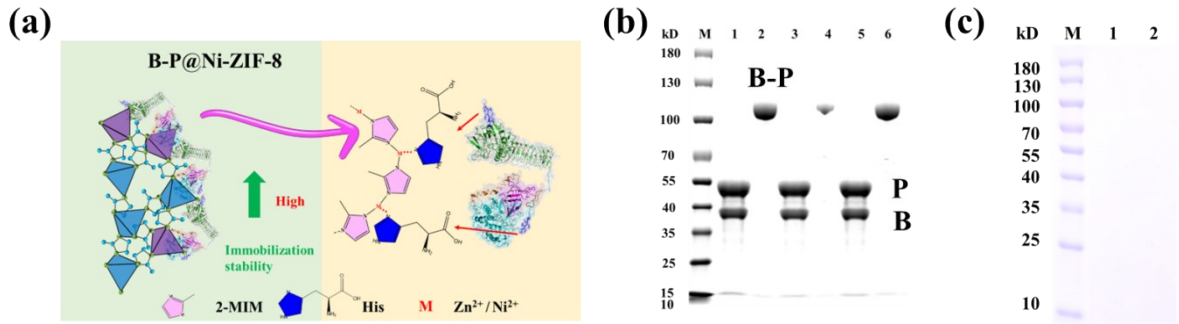

Fig. S12 Scheme of B-P@Ni-ZIF-8 formation through the affinity interaction between the dual-His_6 tag and metals on the surface of MOF (a) Analysis of the interaction between B-P and Ni-ZIF-8 by a elution assay and SDS-PAGE (b) M: marker; 1: B+P; 2: B-P; 3 and 5 are B+P@Ni-ZIF-8 eluted with 100 mM imidazole and 250 mM imidazole respectively.; 4 and 6 are B-P@Ni-ZIF-8 eluted with 100 mM imidazole and 250 mM imidazole respectively; (c) M: marker; Lanes 1 and 2: SDS-PAGE analysis of the enzymes eluted from B+P@Ni-ZIF-8 and B-P@Ni-ZIF-8 by 500 mM NaCl, respectively.

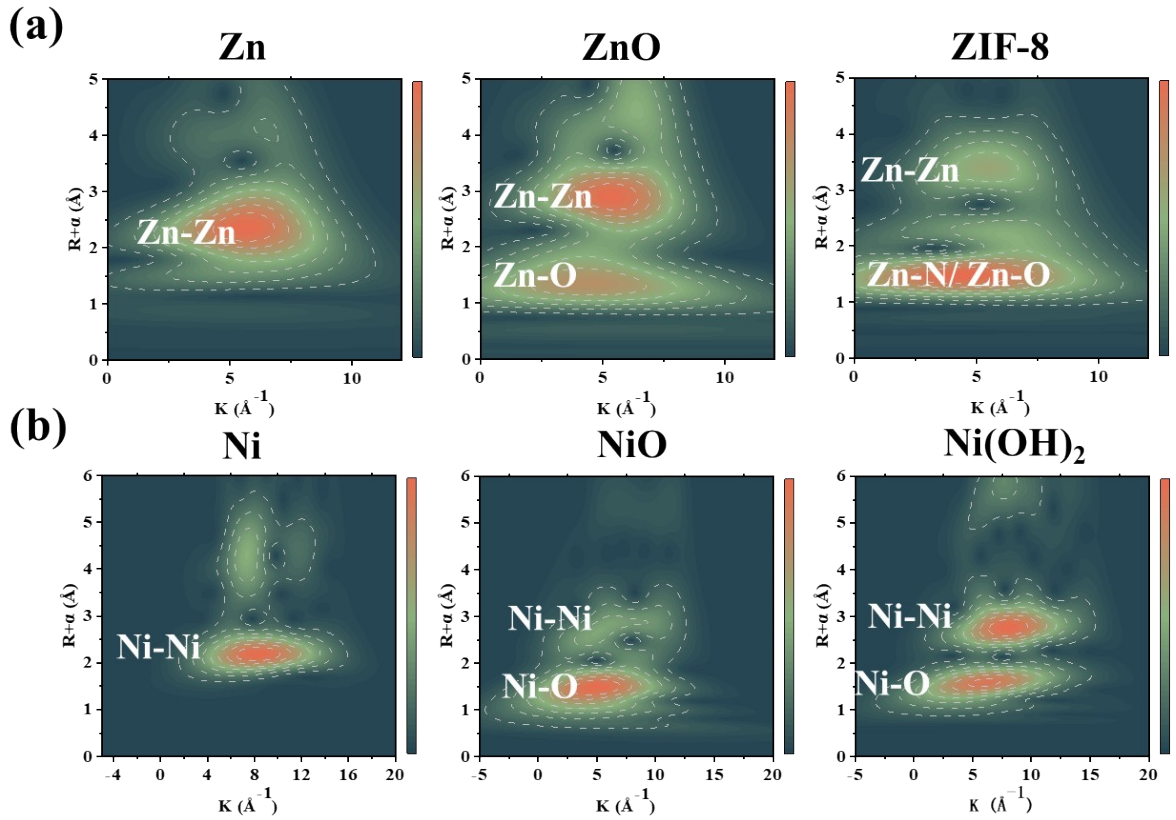

Fig. S13 WT-EXAFS of Zn, Zno and ZIF-8 (a) and Ni, NiO, $NiOH_2$ (b) edges, depicting k-R intensity contours.

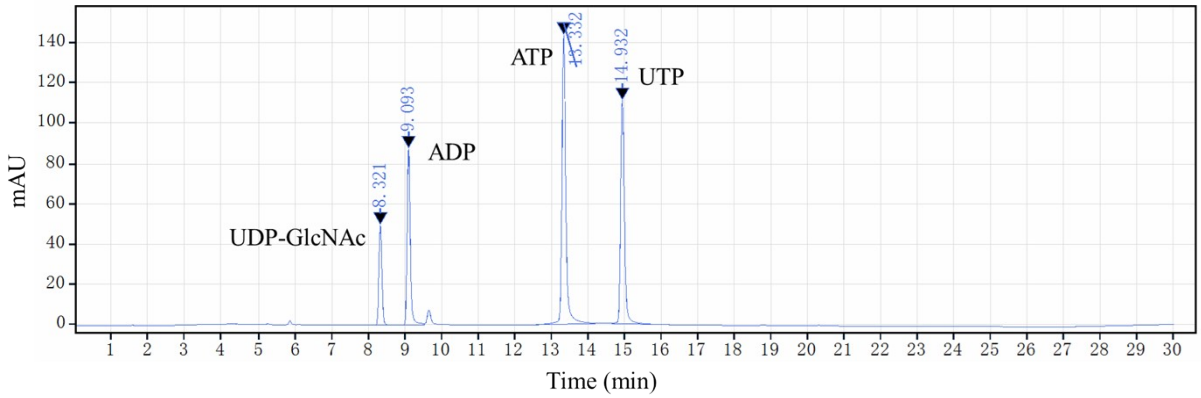

Fig. S14 HPLC chromatograms of ATP, UTP, ADP and UDP-GlcNAc detected at 254 nm.

Table S1 Michaelis-Menten steady-state kinetic parameters

Enzymatic system	ATP			
	K_M / µM	V_{max} / µmol.min^{-1}	k_{cat} / s^{-1}	k_{cat}/K_M / µM^{-1}.s^{-1}
B	0.21	14.32	46.62	220.95
B@Ni-ZIF-8	2.35	15.06	50.15	21.34
B-P@Ni-ZIF-8	1.11	11.32	37.70	33.84
Enzymatic system	**UTP**			
	K_M / µM	V_{max} / µmol.min^{-1}	k_{cat} / s^{-1}	k_{cat}/K_M / µM^{-1}.s^{-1}
P	2.03	26.41	87.94	43.23
P@Ni-ZIF-8	1.37	46.99	156.48	114.30
B-P@Ni-ZIF-8	1.40	44.88	149.45	106.90

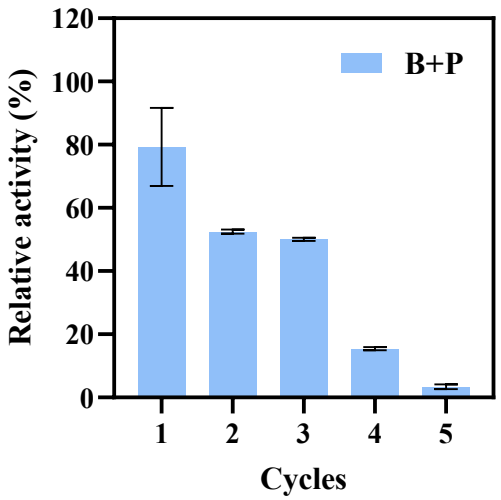

Fig. S15 Recyclability test of free B and P in a dialysis approach. Error bars represent the standard deviation of the mean of duplicate reactions.

Table S2 Representative Strategies Reported for the Enzymatic Production of Sugar Nucleotides

Strategy	GlcNAc, Enzyme concentration	Cycles (activity)	Improved catalytic efficiency	UDP-GlcNAc yield/(time)	References
BlNahK+ PmGlmU+ PmPpA (free enzyme in solution)	GlcNAc (50 to 300 mg, 1.0 eq.), NanK (3.2–4.8 mg), PmGlmU (5–7.5 mg), PmPpA (2.5–5 mg),	/	/	81% (24 to 48 h)	[1]
trGlmU–NahK (enzyme fusion)	GlcNAc (25 mM), trGlmU–NahK (12.55 μM)	/	/	77% (12 h)	[2]
BlNahK@ECR8309F and MtGlmU@EziG™ (enzymes immbolization and flow chemistry)	GlcNAc (8 mM), BiNahK (1.64 mg mL), MtGlmU (0.4 mg mL)	(Batch)/	STY: 0.096 g L^{-1} h^{-1}	95% (48 h)	[3]
		(Flow) 4 cycles (>50%)	STY: 1.90 g L^{-1} h^{-1}	54% (83 min)	
NahK-GlmU@ZIF-90A@PPK (enzyme encapsulation/co-factor regenaration)	GlcNAc (10 mM), NahK (0.5 mg/ mL), GlmU (0.5 mg/ mL), PPK (0.48 mg/ mL)	/	1.4-fold	98% (48 h)	[4]
PSK (PpAmgK, SeGlmU and SePPK)-(G4S)3-CipA (protein scaffolding)	GlcNAc (50 mM), Each enzyme was 5 μM	5 cycles (>60%)	1.65-fold	57% (90 min)	[5]
BlNahK-PmGlmU@Ni-ZIF-8 (spatial organization on surface of Ni-ZIF-8)	GlcNAc (2 mM), Each enzyme was 5 μM	5 cycles (>60%)	4.4-fold	92% (30 min)	This work

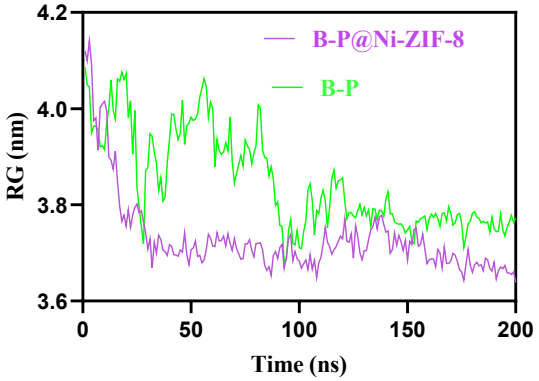

Fig. S16 Radius of gyration (RG) analysis of B-P dual enzyme conjugate in B-P@Ni-ZIF-8 (pink) and in solution (green).

Table S3 The total free energy decomposition profile in the presence and absence of MOF

	In the presence of MOF						
	VDWAALS	EEL	EGB	ESURF	GGAS	GSOLV	TOTAL
ATP	-41.37	-150.82	170.45	-8.63	-192.19	161.82	-30.37
GlcNAc	-45.21	-160.15	180.33	-9.07	-205.36	171.26	-34.1
GlcNAc-1-P	-41.58	-155.92	174.64	-8.84	-197.5	165.8	-31.7
UTP	-51.43	-170.65	196.15	-10.06	-222.08	186.09	-35.99
	In the absence of MOF						
	VDWAALS	EEL	EGB	ESURF	GGAS	GSOLV	TOTAL
ATP	-38.24	-115.73	140.52	-7.31	-153.97	133.21	-20.76
GlcNAc	-37.65	-110.28	135.84	-7.12	-147.93	128.72	-19.21
GlcNAc-1-P	-40.87	-105.91	130.47	-6.95	-146.78	123.52	-23.26
UTP	-36.67	-130.37	142.73	-9.85	-167.04	132.88	-34.16

Note: The table summarizes the decomposition of binding energy (in kcal/mol) for ATP, GlcNAc, GlcNAc-1-P, and UTP with B-P in the presence (above) and absence (below) of MOF.

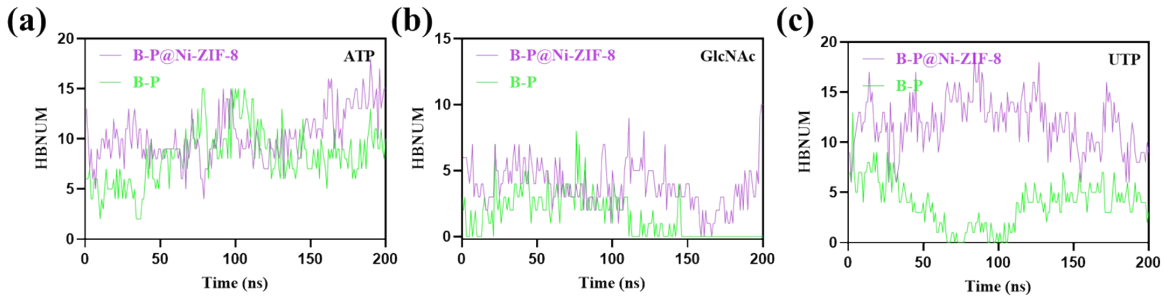

Fig. S17 Hydrogen bong number analysis of between B-P and different substrates including ATP (a), GlcNAc (b), UTP (c) with (pink) and without Ni-ZIF-8 incorporation (green).

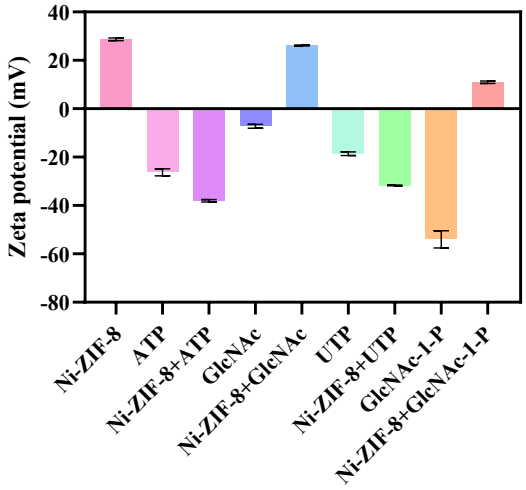

Fig. S18 Zeta potential diagrams of Ni-ZIF-8 in the absence and presence of ATP, GlcNAc, UTP and GlcNAc-1-P, Error bars represent the standard deviation of the mean of triplicate samples.

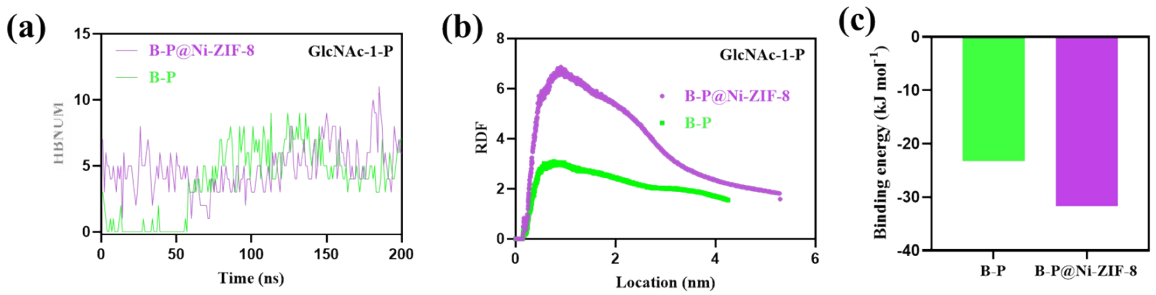

Fig. S19 HBNUM (a), RDF (b) and binding enegey (c) analysis of GlcNAc-1-P and the B-P dual-enzyme conjugate with (pink) and without Ni-ZIF-8 (green).

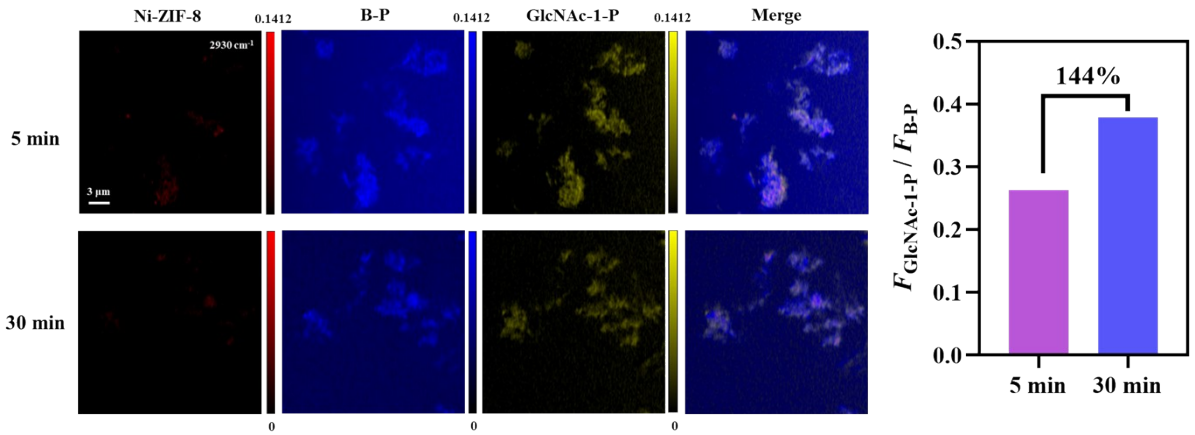

Fig. S20 In-situ analysis of GlcNAc-1-P consumption on B-P@Ni-ZIF-8 surface with free PmGlmU and UTP added in the solution.

Table S4 Primers used for this study

Name	Sequences (5'-3')
SnoopCatcher_ fwd	GGTGGTAGCGGTTCTGGATCCACCGAAAGCAATGAAGTTTTATTC
SnoopCatcher_ rev	GTTAGCCGGGCTACCGAATTCCCTGGCAGCCTCCATGATG
PmGlmU-SnoopTag_fwd	GGAATTCCATATGCACCACCACCACCATCACAAAGAGAAAGCATTAAGTATCG TG
PmGlmU-SnoopTag_rev	CCGCTCGAGTTA**TTTGTTCACTTTAATAAATTCAATATCGCCCAGTTT**CTTTTT CG

Note: The sequences for SnoopCatcher_fwd / SnoopCatcher_rev and PmGlmU-SnoopTag_fwd / PmGlmU-SnoopTag_rev were flanked by restriction sites **BamH*I / *EcoR*I * and * *Nde*I /*XhoI**, respectively. The bolded segments denote the SnoopTag gene.

References

1. Chen, Y., et al., *One-pot three-enzyme synthesis of UDP-GlcNAc derivatives.* Chem Commun (Camb), 2011. **47**(38): p. 10815-7.
2. Zhai, Y., et al., *NahK/GlmU fusion enzyme: characterization and one-step enzymatic synthesis of UDP-N-acetylglucosamine.* Biotechnology Letters, 2012. **34**(7): p. 1321-1326.
3. Roberts, T.L., et al., *A modular, reusable biocatalytic flow system for UDP-GlcNAc production.* Reaction Chemistry & Engineering, 2025. **10**(6): p. 1221-1226.
4. Zheng, J., et al., *Spatially Segregated MOF Bioreactor Enables Versatile Modular Glycoenzyme Assembly for Hierarchical Glycan Library Construction.* ACS Applied Materials & Interfaces, 2023. **15**(16): p. 19807-19816.
5. Li, J., et al., *Construction of immobilized enzyme cascades for the biosynthesis of nucleotide sugars UDP-N-acetylglucosamine and UDP-glucuronic acid.* Systems Microbiology and Biomanufacturing, 2024. **4**(3): p. 895-905.